Journal Pre-proofs

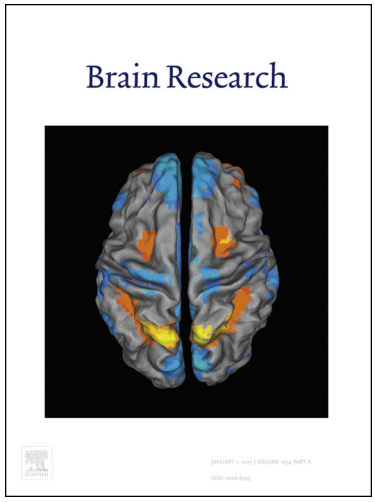

Research report

EGb761 ameliorates cell necroptosis by attenuating RIP1-mediated mitochondrial dysfunction and ROS production in both *in vivo* and *in vitro* models of Alzheimer's disease

Wei-Ping Chen, Zhi-Juan Cheng, Ge Zhang, Qing-Hua Luo, Ming Li, Jiang-Long Tu, Xu Liu

PII: S0006-8993(20)30086-X
DOI: https://doi.org/10.1016/j.brainres.2020.146730
Reference: BRES 146730

To appear in: *Brain Research*

Received Date: 18 September 2019
Revised Date: 18 January 2020
Accepted Date: 13 February 2020

Please cite this article as: W-P. Chen, Z-J. Cheng, G. Zhang, Q-H. Luo, M. Li, J-L. Tu, X. Liu, EGb761 ameliorates cell necroptosis by attenuating RIP1-mediated mitochondrial dysfunction and ROS production in both *in vivo* and *in vitro* models of Alzheimer's disease, *Brain Research* (2020), doi: https://doi.org/10.1016/j.brainres.2020.146730

EGb761 ameliorates cell necroptosis by attenuating RIP1-mediated mitochondrial dysfunction and ROS production in both *in vivo* and *in vitro* models of Alzheimer's disease

Running title: Gingko extract for AD model treatment

Wei-Ping Chen[1], Zhi-Juan Cheng[1], Ge Zhang[2], Qing-Hua Luo[1], Ming Li[1], Jiang-Long Tu[1,*], Xu Liu[1,*]

[1]Department of Neurology, the Second Affiliated Hospital of Nanchang University, Nanchang 330006, P. R. China

[2]Department of Psychiatry, JiangXi Mental Hospital, Nanchang 330029, P.R.China

[*]**Corresponding author:** Dr. **Xu Liu & Jiang-Long Tu**, Department of Neurology, the Second Affiliated Hospital of Nanchang University, No.1, Minde Road, Nanchang 330006, Jiangxi Province, P.R.China.

Email: liuxu9904@163.com; tujianglong32@163.com

Tel: +86-0791-86311759

Abstract

Objectives: To investigate the neuroprotective effect of Gingko biloba extract 761 (EGb761) in Alzheimer's disease (AD) models both *in vivo* and *in vitro* and the underlying molecular mechanism.

Methods: Cultured BV2 microglial cells were treated with $A\beta_{1-42}$ to establish an *in vitro* AD model. The *in vivo* rat AD model was established by injecting $A\beta_{1-42}$. Cells were pre-treated with EGb761, and the proliferation and necroptosis were examined by MTT or flow cytometry assays, respectively. In addition, the membrane potential and oxidative stress were measured. Cognitive function was evaluated by the Morris water maze, and the activation of the JNK signaling pathway was quantified by Western blotting.

Results: Cultured BV2 cells exhibited prominent cell death after $A\beta_{1-42}$ induction, and this cell death was alleviated by EGb761 pre-treatment. EGb761 was found to relieve oxidative stress and suppress the membrane potential and calcium overload. EGb761 treatment in AD model rats also improved cognitive function deficits. Both cultured microglial cells and the rat hippocampus exhibited activation of the JNK signaling pathway, and EGb761 relieved this activation in cells.

Conclusion: Our results showed that EGb761 regulated cell proliferation, suppressed necroptosis and apoptosis, relieved mitochondrial damage, and ameliorated tissue damage to improve cognitive function in AD models. All of these effects may involve the suppression of the JNK signaling pathway.

Keywords: Cell necroptosis; Cultured microglial cells; Neurodegenerative disease; Intracellular signaling pathway

Introduction

Alzheimer's disease (AD) is a neurodegenerative disorder characterized by the extracellular deposition of amyloid beta-protein (Aβ) plaques and intracellular fibrillary tangles caused by the over-phosphorylation of the intracellular tau protein. A recent epidemiology study showed that AD has a 0.625% prevalence in China and is the most prominent cause of dementia in people over the age of 65 [1-3]. Due to its heavy burden on families and public health, AD pathogenesis and treatment are repeatedly investigated. However, controversial results have made the precise pathogenic factors underlying most AD cases unclear. Studies on treatments for AD have mainly focused on the development of molecular targets or drugs for protecting neurons or glial cells from disease-induced cell death.

Necroptosis is a type of caspase-independent programmed cell death that features both necrosis and apoptosis. Necroptosis is known to be mediated by the receptor-interacting protein kinase (RIPK) family [4, 5]. After necroptosis is induced by an extracellular signal, mitochondrial respiration is suppressed, and this process is accompanied by dysregulated intracellular calcium signaling [6, 7], which further leads to oxidative stress (OS) in mitochondria and cell death [8]. A recent study showed the RIPK1 and RIPK3 activation is involved in the AD-related transcriptional profile and that AD severity can be alleviated in a mouse model by suppressing necroptosis [9]. Therefore, the investigation of the mechanism of necroptosis in AD pathogenesis may help develop new targets for neuroprotection and disease treatment.

Ginkgo biloba extract 761 (EGb761) mainly consists of flavone and bilobalide compounds [10]. A previous *in vitro* study showed that EGb761 can protect against Aβ-related cytotoxicity [11]. Multi-center, double-blind, placebo-controlled and randomized clinical trials have provided evidence that disease conditions are improved after the consumption of EGb761 [12]. It is believed that,

mechanistically, EGb761 can help relieve cell apoptotic damage and protect against necrosis [13]. In addition, it has been shown to ameliorate mitochondrial OS damage by suppressing downstream apoptosis signaling in an AD model [14]. However, no study investigating the protective role of EGb761 against AD from the perspective of necroptosis has been performed.

In this study, we employed both an *in vitro* cell culture model of AD and an *in vivo* AD rat model to study the regulation of Aβ-induced necroptosis by EGb761 and related functions in AD pathogenesis. We found that EGb761 can suppress the JNK signaling pathway both *in vivo* and *in vitro* and that this mechanism may underlie the protective effects of EGb761 against Aβ-induced cell death and tissue morphology, as well as the protective effects of EGb761 against cell apoptosis and cell necroptosis in BV2 cells and improve cognitive function. Our results provide evidence for using plant extracts to treat neurodegenerative diseases.

Results

1. EGb761 treatment suppressed $A\beta_{1-42}$-induced cell death and enhanced cell viability in BV2 cells

Firstly, we determined effects of different concentrations of $A\beta_{1-42}$ on cell viability of BV2 cells. As shown in Figure 1A, the cell viability was remarkably reduced by treatment of $A\beta_{1-42}$ and the effect was in a dose-dependent manner. Then we performed a pilot study to examine whether EGb761 pre-treatment can ameliorate the Aβ-induced decrease in the viability of microglial cells. We used serial concentrations of EGb761 (0, 25, 50, 100 and 200 μg/ml) and measured cell viability by the MTT assay at 24 h. The results showed that 50 μg/ml EGb761 had the most significant effect on suppressing the 10 μM $A\beta_{1-42}$--induced decrease in cell viability (Figure 1B). To further determine the effects of EGb761 on Aβ-induced cells, different concentrations of EGb761 (0, 25, 50, 100 μg/ml) were used to treat the cells which was pre-treated by 10 μM $A\beta_{1-42}$. We found that both 50 and 100 μg/ml EGb761 could significantly increase the cell viability, which was reduced by $A\beta_{1-42}$ (Figure 1C).

We then used flow cytometry to quantify the effect of EGb761 on cell death. Flow cytometry using annexin-V/PI staining showed that 10 μM $A\beta_{1-42}$-treated BV2 cells exhibited a significantly higher mortality ratio than that of the control group (29.24% vs 3.30%, $p<0.05$, Figure 1D and 1E), while EGb761 (50 μg/ml) pre-treatment remarkably suppressed 10 μM $A\beta_{1-42}$-induced cell death (9.87%, $p<0.05$). Therefore, EGb761 pre-treatment effectively protected cultured microglial cells from $A\beta_{1-42}$-induced cell death and enhanced cell viability.

2. EGb761 treatment ameliorated $A\beta_{1-42}$-induced mitochondrial damage

Mitochondrial damage is a widely known pathology mechanism of AD. In this study, we measured the mitochondrial membrane potential (MMP), which was depressed after $A\beta_{1-42}$ treatment (10 μM, Figure

2A and 2B, as suggested by the lower red/green fluorescent ratio). EGb761 intervention (50 μg/ml) effectively reversed this reduction in potential. Similar results were obtained regarding the production of reactive oxygen species (ROS) by mitochondria in all groups of BV2 cells. The results showed that $A\beta_{1-42}$-treated cells exhibited significantly higher ROS levels, as suggested by elevated fluorescence, and pre-treatment with EGb761 effectively suppressed ROS production ($p<0.05$, Figure 2C and 2D). To explain the electrophysiological mechanism underlying the changes in MMP, we measured the Ca^{2+}current and found that $A\beta_{1-42}$ treatment increased the Ca^{2+}current amplitude, and EGb761 treatment corrected such deficits to a large extent (Figure 2E). Besides, we measured protein levels of NCLX, MCUB, MICU1, MICU2, VADC and CV-Sα to investigate effects of EGb761 on mitochondrial calcium efflux. Results showed that treatment of $A\beta_{1-42}$ significantly reduced the expression of NCLX, MCUB and MICU1, and EGb761 remarkably reversed the effects (Figure S1A). However, no significant difference was found for MICU2, VADC and CV-Sα by treatment of $A\beta_{1-42}$ or EGb761. In summary, EGb761 pre-treatment prevented BV2 cells from $A\beta_{1-42}$-induced cell death, possibly via relieving mitochondrial damage.

3. EGb761 likely suppressed RIP1-induced cell necroptosis after $A\beta_{1-42}$ treatment

We further investigated whether EGb761 can similarly alleviate RIP1-induced cell necrosis through $A\beta_{1-42}$ treatment. First, RIP1 shRNA transfection effectively suppressed RIP1 mRNA expression, as determined by RT-qPCR (Figure 3A), confirming the transfection efficiency. Next, we used flow cytometry to measure cell necroptosis 36 h and 48 h after treatment with $A\beta_{1-42}$ (10 μM) and found that, compared to the shNC control, shRIP effectively decreased the percentage of cell necroptosis (Figure 3B). Moreover, EGb761 treatment (25~100 μg/ml) also alleviated cell necroptosis in both shNC- and shRIP1-transfected cells (Figure 3C) in an approximately dose-dependent manner. We next

determined whether $A\beta_{1-42}$ is involved in this process by administering the necroptosis inhibitor Necrostatin-1 (Nec-1); it was found that Nec-1 suppressed $A\beta_{1-42}$-induced cell death, especially at high doses (Figure 3D), suggesting that $A\beta_{1-42}$ (10 μM) can lead to cell necroptosis. Flow cytometry was then used to measure cell death after the administration $A\beta_{1-42}$ and/or EGb761 (50 μg/ml) plus Nec-1. The results showed that $A\beta_{1-42}$ remarkably induced cell death and that this effect was alleviated by EGb761 or Nec-1 treatment. EGb761 and Nec-1 seemed to have a synergistic effect on antagonizing $A\beta_{1-42}$ induced cell death (Figure 3E). We also found that treatment of Cyclosporin A (CsA) remarkably reduced cell death and could show synergistic effects with EGb761 (Figure S1B). These data suggested that EGb761 alleviated $A\beta_{1-42}$-induced necroptosis and apoptosis. Finally, we measured the effect of gradient concentrations of EGb761 on RIP1 proteins and found that RIP1 protein expression gradually decreased as the RIP1 concentration increased, indicating that EGb761 can suppress cell necroptosis.

4. EGb761 suppressed the JNK signal pathway

To investigate the possible signaling pathways involved in EGb761-mediated cell protective effects, we used Western blotting to evaluate JNK pathway activation by measuring the protein levels of JNK, TNF-α, RIP1, p-STAT3 (Ser 727), PGAM5, MLKL and p-MLKL. The results showed that, compared to $A\beta_{1-42}$ treatment (10 μM), EGb761 intervention (50 μg/ml) remarkably suppressed the activation of the JNK pathway, as indicated by the decreased phosphorylation levels of JNK and STAT3 effector proteins and lower protein levels of TNF-α, RIP1, p-STAT3 (Ser 727), PGAM5, MLKL and p-MLKL (Figure 4A and 4B). To further substantiate this model, we treated BV2 cells with the JNK agonist anisomycin and found that anisomycin treatment effectively antagonized the effect of EGb761 on the

JNK pathway (Figure 4A and 4B). This evidence collectively suggests that EGb761 can suppress the JNK signaling pathway, the activation of which is possibly involved in $A\beta_{1-42}$-induced cell damage.

5. EGb761 improved the cognitive function of AD model rats

To investigate the effect of EGb761 *in vivo*, we utilized a rat model of AD. The rats were first allowed to freely explore the space with a hidden platform. The results showed that, during the navigation session, the AD model rats exhibited a significantly longer latency to locate the platform, and EGb761 treatment (20 mg/kg daily) partially rescued this deficit in cognitive function (Figure 5A, $p<0.05$). In the spatial probe test, the platform was removed, and the average swimming speed and number of target platform crossings were recorded. The results showed that AD model rats exhibited a slower swimming speed and a lower number of target platform crossings, and both of these parameters were increased by EGb761 treatment (Figure 5B and 5C, $p<0.05$). Therefore, EGb761 can protect against Aβ-induced cognitive function deficits.

6. EGb761 modulated JNK signaling pathway activity *in vivo*

To fully elucidate the effect of EGb761 on the JNK signaling pathway in AD model rats, we treated rats with EGb761 and performed IHC on hippocampal tissue slices. As shown in Figure 6A-B, $A\beta_{1-42}$ was detected in the rat hippocampus, and treatment with $A\beta_{1-42}$ significantly enhanced its expression while EGb761 markedly reversed this effect. While AD rats exhibited prominent cell death in the CA1 region, EGb761 treatment remarkably alleviated cell death and restored normal tissue morphology (Figure 6A). We further extracted total protein from the hippocampal CA1 region of AD model rats and employed a series of Western blotting assays to study the expression of the downstream effectors of this pathway. Consistent with the *in vitro* data, our results showed that AD model rats presented

significantly elevated phosphorylation levels of JNK and STAT3 and higher protein levels of RIP1, MLKL and p-MLKL. The administration of EGb761 (20 mg/kg daily) partially relieved the overactivation of the JNK signaling pathway, as shown by the suppressed phosphorylation of JNK and STAT3 and the lower levels of RIP1, MLKL and p-MLKL (Figure 6C and 6D). In summary, AD model rats exhibited activation of the JNK signaling pathway, which was rescued by EGb761; this may represent the molecular mechanism underlying improvements in cognitive function deficits.

Discussion

AD has become a major health concern in elderly people because it carries heavy burdens for both the patient's family and the public health system. The treatment of AD with extracts from natural plants has received much attention in recent years. The Gingko biloba extract EGb761 has been demonstrated to exert neuroprotective effects in AD patients [15]. A recent study in which AD mice were treated with EGb761 found that it can improve cognitive function, such as performance in the Barnes Maze test, and rescue the loss of synaptic proteins, such as PSD-95 [16]. More specifically, EGb761 was found to inhibit Aβ aggregation and to attenuate cell apoptosis in a transgenic cell model [17]. We thus employed an Aβ-induced BV2 cell model to test the effect of EGb761 in cells and found similar results; EGb761 pre-treatment effectively reduced Aβ-induced cell death. Therefore, EGb761 has potent cell protective effects.

Microglial cells are considered as an important component in AD development. The activation of microglial cells can result in series of inflammatory response, including alteration of cell morphology, immunophenotype and function, release of inflammatory factors like IL-1, TNF-α and NO. In an early study, it was observed that numerous microglial cells were stained intensively in AD tissues [18]. Recent researches also demonstrated that microglial cells were activated in AD patients and inflammatory factors directly released by microglial cells and indirectly released by endothelial cells might lead to systematic inflammation and might attract monotypes and T lymphocytes to the central nervous system [19, 20]. In the present research, we used an *in vitro* AD model of human microglial cell line BV2 cells treated with $A\beta_{1\text{-}42}$ to investigate the effects of EGb761 on AD cells, which might help further understanding the function of microglial cells in AD.

Cell necrosis can be mediated by various endogenous and exogenous factors. Among these, mitochondrial damage is a critical endogenous initiator. In AD pathogenesis, oxidative stress and

mitochondrial dysfunction play critical roles; for example, functionally damaged mitochondria can produce reactive oxygen species (ROS) and less energy, leading to cellular dysfunction and necrosis [21]. Besides, the treatment of Aβ can induce cell necrosis in U-937 cells [22], and this process is associated with many signaling pathways, such as alteration of ATP channel and Ca channel, activation of oxidative stress and N-methyl-D-aspartate receptors, etc [23, 24]. The induction of cell death by RIP1 was reported in many researches [25, 26]. And Necrostatin-1 could improve cell death by inhibition of RIP1 signaling [27]. In this study, we found that EGb761 pre-treatment protected mitochondria from external damage and EGb761 also reduced RIP1-induced cell necroptosis, which could be also suppressed by Nec-1. We also investigated the role of calcium overloading, which is an important cause of mitochondrial dysfunction [28], in AD pathogenesis and the effects of EGb761. For the first time, we reported an elevated calcium current and a higher MMP in a cell model of $A\beta_{1-42}$-induced AD, and pre-treatment with EGb761 effectively reversed the mitochondrial calcium overload and oxidative stress. These results elucidate the role of mitochondria dysfunction in an AD cell model and identify EGb761 as a target.

In an AD rat model, we successfully restored cognitive function by administering EGb761. This phenotype was accompanied by improved cell survival and status in the hippocampal CA1 region. These results are in line with those of our early *in vitro* assay, which showed enhanced proliferation and decreased necrosis in cultured BV2 cells pre-treated with EGb761 before $A\beta_{1-42}$ challenge. Our findings are consistent with a similar finding that EGb761 can improve the cognition and memory of AD rats [29]. However, no consensus has been reached regarding the molecular mechanism by which EGb761 alleviates AD symptoms. Previous findings have postulated various mechanisms, including the alleviation of oxidative stress [30], the regulation of the inflammatory response [31], and the prevention of amyloid aggregation and apoptosis [32] or endoplasmic reticulum stress [33]. These

mechanisms mainly involve cell stress and the microenvironment but largely neglect intracellular molecular mechanisms.

The JNK signaling pathway is widely involved in multiple cell behaviours. In an AD-related study, the JNK pathway was found to mediate cell necrosis [34]. Besides, it was found chronic activation of JNK/ JAK/STAT signaling might result in the loser cell status [35]. In another research, authors also considered JNK as a potential therapeutic target for AD [36]. We thus quantified the phosphorylation of JNK proteins and their downstream effectors. *In vitro* and *in vivo* assays both showed that Aβ aggregation induced the prominent activation or phosphorylation of JNK proteins. As the activation of JNK is strongly related to the induction of cell death by the production of inflammatory factors, such as TNF-α [37], it is thus proposed that JNK activation leads to hippocampal cell necrosis by through an inflammatory niche. We also investigated the role of STAT3 downstream of JNK. A previous study found that JNK-STAT3 activation results in mitochondrial stress in microglial cells [38]. In this study, we found elevated STAT3 phosphorylation in $A\beta_{1-42}$-challenged BV2 cells and in a rat model, thus providing an explanation for mitochondrial damage in the AD model. Upon the administration of EGb761, we found consistent results in both cells and rat hippocampal tissues; EGb761 suppressed JNK-STAT3 activation. Moreover, the necrosome proteins RIP1 and MLKL were found to mediate stress-induced cell death, including apoptosis and necroptosis [39]. This study also revealed the possible involvement of RIP1 and MLKL in AD-related necrosis and provided evidence for the alleviating effects of EGb761. All of these pieces of evidence support the role of EGb761 in alleviating Aβ-induced cell stress and consequently necrosis in cells.

This study also has some limitations. First, the time course of treatment effects of EGb761 on JNK signaling is unclear. Secondly, effects of different doses of EGb761 on JNK signaling also needs further studies to confirm. Thirdly, the long-term cognitive functions of EGb761 is also unclear.

Fourthly, more cell types not only microglial cells should be used to confirm the results of this study in the future.

In summary, we provided both *in vitro* and *in vivo* data showing that EGb761 can rescue microglial cells from $A\beta_{1\text{-}42}$-induced cell stress, necrosis, thus relieving tissue damage and improving cognitive function, which could be seen in the schematic figure (Figure 7), explicitly illustrating the working model. Our results may help to illustrate the mechanism by which EGb761 can treat AD and propose the use of EGb761 for treating other neurodegenerative and neurological diseases.

Materials and Methods

1. Microglial cell culture and the MTT assay

A human microglial cell line (BV2) was cultured in DMEM with 10% foetal bovine serum (FBS) in a 37°C chamber with 5% CO_2. Lyophilized human $A\beta_{1-42}$ (Sigma-Aldrich, USA) was diluted to 1 mM in DMSO. The cells were then treated with $A\beta_{1-42}$ with different concentrations. (0.1 μM, 1 μM, 5 μM, 10 μM). Untreated cells were used as control. For the EGb761 treatment group, cells were pre-treated with gradient concentrations (25, 50, 100 and 200 μg/ml) of EGb761 (in DMSO) for 2 h and were then treated with 10 μM $A\beta_{1-42}$.

Cell viability was measured by the MTT assay. In brief, BV2 cells from all groups were seeded in 96-well plates and treated with EGb761 (Blackmore, Australia) and/or $A\beta_{1-42}$. Then, 20 μl of MTT (5 mg/ml stock) was added to each well containing 100 μl of medium. After 4 h of incubation at 37°C, the culture medium was removed. Then, 100 μl of DMSO was added to each well to dissolve the crystal. The absorbance value at 490 nm was measured by a microplate reader (Bio-Rad, Hercules, CA, USA). Relative viability was expressed as the ratio of the viability of the treated cells relative to that of the control group.

2. Preparation of $A\beta_{1-42}$

Briefly, $A\beta_{1-42}$ peptide powder, which was purchased from Sigma-Aldrich, St. Louis, MI, USA, was mixed with hexafluoroisopropanol (Sigma-Aldrich). The solution was diluted to 10 mmol/l with DMSO and further diluted to 1 mmol/l with DMEM. After incubation for 72 h at 37°C, the solution was further incubated at 4°C for 1 week and stored at -80°C.

3. Flow cytometry for the measurement of cell necrosis

BV2 cells from each group were digested by trypsin and re-suspended in PBS. Then, 5 μl of annexin V-FITC and 5 μl of PI solution (BD, USA) were added, followed by a 15-min incubation at room temperature. The death of the cells was determined by a BD FACS Calibur (BD Biosciences, San Diego, CA, USA) at a wavelength of 488 nm.

4. Assay for ROS activity in cultured cells

BV2 cells from all groups were treated as mentioned above and were incubated in 2.5 μM MitoSOX Red reagent for 10 min. After washing, the fluorescence was measured for 30 min at 510 nm excitation and 580 emission wavelengths using a LS50B Luminescence spectrophotometer (Perkin, USA). Superoxide production was initiated by the mitochondrial complex I substrates sodium pyruvate and malic acid. The reaction was then quenched by the addition of 1 mM MmTBAP. The production of superoxide was calculated temporally based on the fluorescence per mg.

5. Mitochondrial membrane potential (MMP) assay

The MMP was measured using a JC-1 flow cytometry probe (BD, USA) as previously described [15]. In brief, cells from all groups were co-incubated with 10 μg/ml JC-1 in the dark for 20 min at 37°C. The cells were washed with PBS three times and were imaged under a confocal microscope (Zeiss, Germany). JC-1 exists as a green fluorescent probe (488 nm) at a low MMP and forms red fluorescent aggregates (590 nm) at a high MMP. The MMP can thus be quantified by comparing the 590/488 fluorescent intensity ratio.

6. Fura-2/AM fluorescence assay for the measurement of the Ca^{2+} current

The cytosolic free Ca^{2+} level was determined using the Ca^{2+} indicator dye Fura-2 in a Hitachi spectrofluorimeter (Hitachi, Japan) as described elsewhere [16, 40]. Briefly, the cells were suspended in HBSS and incubated for 1 h with 5 μM Fura-2/AM. Thereafter, the cells were washed twice and resuspended in HBSS, and Fura-2 fluorescence was monitored at 510 nm in a continuously stirred cell suspension at room temperature.

7. Western blotting

Cells from all groups were first treated with the JNK signaling pathway agonist anisomycin and were analysed for protein expression using Western blotting. In brief, the cells were washed twice in PBS. Total protein was extracted by RIPA lysis buffer and then centrifuged at 12,000 x g for 30 min. The protein was quantified by a BCA assay kit, separated by SDS-PAGE (15%), and transferred to an NC membrane. The membrane was first blocked and then incubated in primary antibodies against p-JNK, t-JNK, TNF-α, p-STAT3 (Ser 727), t-STAT3 (Ser 727), PGAM5, RIP1, MLKL, p-MLKL, NCLX, MCUB, MICU1, MICU2, VADC and CV-Sα (1:1000 dilution, Sigma, USA). β-Actin was used as the internal control. The membrane was incubated with primary antibody for 1.5 h and with an enzyme-linked secondary antibody for 2 h at room temperature. In addition, the membrane was incubated with ECL solution (Beyotime, China) and then exposed using an enhanced chemiluminescence Western blotting system (Pierce, Biotechnology Inc., Rockford, USA).

8. AD rat model and Morris water maze test

Adult male Wistar Rats (2 months old, 300-350 g) were housed under a standard 12-h light/dark cycle with food and water *ad libitum*. All animal procedures were approved by the ethics committee of our institute. The AD model was generated by the intracerebroventricular (ICV) injection of the $A\beta_{1-42}$

peptide as previously described [17]. In brief, 10 μg of $A\beta_{1-42}$ peptide was injected into the bilateral ventricles (0.8 mm posterior and 1.5 mm lateral to bregma) using a Hamilton syringe and stereotaxic holder. To determine the protective role of EGb761, the drug was given by gavage (20 mg/kg daily) for 23 days. A parallel sham control group received an equal volume of saline by ICV infusion.

The Morris water maze (MWM) was carried out to test the cognitive function of rats, as described elsewhere [41]. In brief, rats were placed in a circular pool with a diameter of 1.2 m and a depth of 45 cm filled with water (24 ± 1°C). A transparent platform (10 cm in diameter) was placed in one quadrant, and its surface was 2 cm below the water. The rats first underwent acquisition sessions on 5 consecutive days with 4 trials per day per rat. During these trials, the rats were placed in the pool facing the wall and were allowed 60 s to locate the submerged platform. If the animal failed to reach the platform within the prescribed time limit, it was guided to the platform and kept on it for 15 s. After the acquisition phase, the probe test was conducted on day 6; the rats were allowed to swim freely for 60 s without the platform, and the trajectory path was recorded by a camera and analysed by software. The following parameters were recorded: 1) the latency to find the platform, (b) the average swimming speed and (c) the number of target platform crossings. For all animal experiments, each group included 6 rats.

9. Immunohistochemistry (IHC)

Tissues from the right hemisphere were immediately collected after resection, fixed with 4% paraformaldehyde, embedded in paraffin and sectioned. The samples were then treated with 3% H_2O_2, blocked with 10% (v/v) normal goat serum for 45 min, and incubated with a rabbit anti-$A\beta_{1-42}$ antibody (1:100, Abcam, Cambridge, MA, USA) at 4°C overnight. After incubation with a corresponding secondary antibody (goat Anti-rabbit IgG, 1:200, Abcam) at 37°C for 45 min at room temperature, the

samples were stained with diaminobenzidine (DAB). The area of $A\beta_{1-42}$ staining was determined by Image Pro Plus 6.0 (Rasband; NIH, USA).

10. Statistical analysis

All data are presented as the mean ± standard deviation (SD). Parametric data were compared by Student's t-test. For multi-group comparisons, one-way analysis of variance (ANOVA) followed by Tukey's post hoc test was used. Statistical significance was defined as $p < 0.05$. All statistical analyses were performed using SPSS 22.0 software.

Acknowledgements

This work was supported by the Science Foundation for Youths of Jiangxi Province (no. 20171BAB215018); the Youth Science Grant of the Second Affiliated Hospital of Nanchang University (no. 2016YNQN12022); The National natural science foundation of China(grant No.81860212); The jiangxi provincial natural science foundation for youth scientific research(grant No.20192ACBL21038)

Conflict of interest

The authors declare that they have no conflict of interest.

References

1. Chan, K.Y., et al., *Epidemiology of Alzheimer's disease and other forms of dementia in China, 1990–2010: a systematic review and analysis.* Lancet, 2013. **381**(9882): p. 2016-2023.
2. Veitch, D.P., et al., *Understanding disease progression and improving Alzheimer's disease clinical trials: Recent highlights from the Alzheimer's Disease Neuroimaging Initiative.* Alzheimer's & Dementia, 2019. **15**(1): p. 106-152.
3. Selkoe, D.J., *Early network dysfunction in Alzheimer's disease.* Science, 2019. **365**(6453): p. 540-541.
4. Andreas Linkermann, D.R.G., *Necroptosis.* New England Journal of Medicine, 2014. **370**(5): p. 455.
5. Shirjang, S., et al., *MicroRNAs in cancer cell death pathways: Apoptosis and necroptosis.* Free Radical Biology and Medicine, 2019.139:1-15.
6. Claire, T. and H. Henrik, *Role of mitochondria in apoptotic and necroptotic cell death in the developing brain.* Clinica Chimica Acta, 2015. **451**(Pt A): p. 35-38.
7. Fritsch, M., et al., *Caspase-8 is the molecular switch for apoptosis, necroptosis and pyroptosis.* Nature, 2019. **575**(7784): p. 683-687.
8. Mulay, S.R., et al., *Mitochondria permeability transition versus necroptosis in oxalate-induced AKI.* Journal of the American Society of Nephrology, 2019. **30**(10): p. 1857-1869.
9. Caccamo, A., et al., *Necroptosis activation in Alzheimer's disease.* Nature Neuroscience, 2017. **20**(9): p. 1236.
10. Müller, W.E., et al., *Therapeutic efficacy of the Ginkgo special extract EGb761® within the framework of the mitochondrial cascade hypothesis of Alzheimer's disease.* The World Journal of Biological Psychiatry, 2019. **20**(3): p. 173-189.

11. Yuan, L., et al., *Inhibition of amyloid-beta aggregation and caspase-3 activation by the Ginkgo biloba extract EGb761.* Proceedings of the National Academy of Sciences of the United States of America, 2002. **99**(19): p. 12197-12202.

12. Kanowski, S. and R. Hoerr, *Ginkgo biloba extract EGb 761 in dementia: intent-to-treat analyses of a 24-week, multi-center, double-blind, placebo-controlled, randomized trial.* Pharmacopsychiatry, 2003. **36**(06): p. 297-303.

13. Ahlemeyer, B. and J. Krieglstein, *Pharmacological studies supporting the therapeutic use of Ginkgo biloba extract for Alzheimer's disease.* Pharmacopsychiatry, 2003. **36**(S 1): p. 8-14.

14. Tian, X., et al., *The protective effect of hyperbaric oxygen and Ginkgo biloba extract on Aβ25-35-induced oxidative stress and neuronal apoptosis in rats.* Behavioural Brain Research, 2013. **242**(1): p. 1-8.

15. Liu, X., et al., *Resveratrol protects PC12 cells against OGD/R-induced apoptosis via the mitochondrial-mediated signaling pathway.* Acta Biochimica et Biophysica Sinica, 2016. 48(4): p. 342-53.

16. Heringdorf, D.M.Z., et al., *Inhibition of Ca signaling by the sphingosine 1-phosphate receptor S1P.* Cellular Signaling, 2003. **15**(7): p. 677-687.

17. Min, L., et al., *Cognitive improvement of compound danshen in an Aβ25-35 peptide-induced rat model of Alzheimer's disease.* Bmc Complementary & Alternative Medicine, 2015. **15**(1): p. 382.

18. Haga, S., K. Akai, and T. Ishii, *Demonstration of microglial cells in and around senile (neuritic) plaques in the Alzheimer brain.* Acta Neuropathologica, 1989. **77**(6): p. 569-575.

19. Dionisio-Santos, D.A., J.A. Olschowka, and M.K. O'Banion, *Exploiting microglial and peripheral immune cell crosstalk to treat Alzheimer's disease.* Journal of Neuroinflammation, 2019. **16**(1): p. 74.

20. Taipa, R., et al., *Patterns of Microglial Cell Activation in Alzheimer Disease and Frontotemporal Lobar Degeneration.* Neurodegenerative Diseases, 2017: p. 145-154.

21. Shi, C., et al., *Ginkgo biloba Extract in Alzheimer's Disease: From Action Mechanisms to Medical Practice.* International Journal of Molecular Sciences, 2010. **11**(1): p. 107-123.

22. Currie, J.R., et al., *Reduction of histone toxicity by the Alzheimer β-amyloid peptide precursor.* Biochimica Et Biophysica Acta Molecular Cell Research, 1997. **1355**(3): p. 248-258.

23. Chi, X., et al., *Potassium channel openers prevent β-amyloid toxicity in bovine vascular endothelial cells.* Neuroscience Letters, 2000. **290**(1): p. 9-12.

24. Morkuniene, R., et al., *Small Aβ1–42 oligomer-induced membrane depolarization of neuronal and microglial cells: Role of N-methyl-D-aspartate receptors.* Journal of Neuroscience Research, 2015. **93**(3): p. 475-86.

25. Thapa, R.J., et al., *NF-κB Protects Cells from Gamma Interferon-Induced RIP1-Dependent Necroptosis.* Molecular & Cellular Biology, 2011. **31**(14): p. 2934-2946.

26. LaRocca, T.J., et al., *Hyperglycemic conditions prime cells for RIP1-dependent necroptosis.* Journal of Biological Chemistry, 2016. 291(26):p. 13753-61.

27. Su, X., et al., *Necrostatin-1 Ameliorates Intracerebral Hemorrhage-Induced Brain Injury in Mice Through Inhibiting RIP1/RIP3 Pathway.* Neurochemical Research, 2015. **40**(4): p. 643-650.

28. Liu, X., et al., *Long-term treatment with Ginkgo biloba extract EGb 761 improves symptoms and pathology in a transgenic mouse model of Alzheimer's disease.* Brain Behavior & Immunity, 2015. **46**: p. 121-131.

29. Wang, X., et al., *Oxidative stress and mitochondrial dysfunction in Alzheimer's disease ☆.* Biochim Biophys Acta, 2014. **1842**(8): p. 1240-1247.

30. Gaetano, S., et al., *Mitochondrial calcium overload is a key determinant in heart failure.* Proc Natl Acad Sci U S A, 2015. **112**(36): p. 11389-11394.

31. Zhang, L.D., et al., *Hyperbaric Oxygen and Ginkgo Biloba Extract Ameliorate Cognitive and Memory Impairment via Nuclear Factor Kappa-B Pathway in Rat Model of Alzheimer's Disease.* Chinese Medical Journal, 2015. **128**(22): p. 3088-3093.

32. Xiaoqiang, T., et al., *Hyperbaric oxygen and Ginkgo Biloba extract inhibit Aβ25-35-induced toxicity and oxidative stress in vivo: a potential role in Alzheimer's disease.* International Journal of Neuroscience, 2012. **122**(10): p. 563-569.

33. Wan, W., et al., *EGb761 improves cognitive function and regulates inflammatory responses in the APP/PS1 mouse.* Experimental Gerontology, 2016. **81**: p. 92-100.

34. Liu, L., et al., *EGb761 protects against Aβ 1-42 oligomer-induced cell damage via endoplasmic reticulum stress activation andHsp70 protein expression increase in SH-SY5Y cells.* Experimental Gerontology, 2016. **75**: p. 56-63.

35. Kucinski, I., et al., *Chronic activation of JNK JAK/STAT and oxidative stress signaling causes the loser cell status.* Nature communications, 2017. **8**(1): p. 136.

36. Yarza, R., et al., *c-Jun N-terminal kinase (JNK) signaling as a therapeutic target for Alzheimer's disease.* Frontiers in pharmacology, 2016. **6**: p. 321.

37. Rumana, A., et al., *The regulation of p53 up-regulated modulator of apoptosis by JNK/c-Jun pathway in β-amyloid-induced neuron death.* Journal of Neurochemistry, 2015. **134**(6): p. 1091.

38. Galina, D. and I. Dmitry, *Tumor necrosis factor-alpha mediates activation of NF-κB and JNK signaling cascades in retinal ganglion cells and astrocytes in opposite ways.* European Journal of Neuroscience, 2014. **40**(8): p. 3171-3178.

39. Zhihong, G., et al., *Leptin-mediated cell survival signaling in hippocampal neurons mediated by JAK STAT3 and mitochondrial stabilization.* Journal of Biological Chemistry, 2008. **283**(3): p. 1754.

40. Meng, X.-L., et al., *Selenoprotein SELENOK enhances the migration and phagocytosis of microglial cells by increasing the cytosolic free Ca2+ level resulted from the up-regulation of IP3R.* Neuroscience, 2019. **406**: p. 38-49.

41. An, J., et al., *Exenatide alleviates mitochondrial dysfunction and cognitive impairment in the 5× FAD mouse model of Alzheimer's disease.* Behavioural brain research, 2019. **370**: p. 111932.

Figure Legends

Figure 1 EGb761 alleviated cell apoptosis. (A) Dose-dependent changes in cell viability by $A\beta_{1-42}$ treatment were determined by the MTT assay. (B) Dose-dependent changes in cell viability by EGb761 treatment were determined by the MTT assay. (C) The temporal pattern of the alleviation of the Aβ-42-induced decrease in cell viability by EGb761 was determined by the MTT assay. (D) Cell flow cytometry was conducted to evaluate cell death after EGb761 treatment. (E) Quantification of (C). *$p < 0.05$, **$p < 0.01$ compared to the control group.

Figure 2 EGb761 reversed mitochondrial damage. (A) The mitochondrial membrane potential was measured by the fluorescence ratio. (B) Quantification of (A). (C) Immunofluorescence staining was performed to measure intracellular ROS levels. (D) Quantification of (C). (E) The density of the mitochondrial transient calcium current was also calculated by the Fura-2/AM fluorescence assay. *$p < 0.05$, **$p < 0.01$ compared to the control group.

Figure 3 EGb761 alleviated cell necroptosis. (A) The transfection efficiency of shRIP1 in BV2 cells was determined using both RT-qPCR and Western blotting. (B) Flow cytometry was used to determine the cell necroptosis rate after shRIP1 transfection. (C) Flow cytometry quantification was performed to determine the cell necroptosis rate after treatment with gradient concentrations of EGb761. (D) The effect of Nec-1 on the $A\beta_{1-42}$-induced decrease in cell viability was measured by the MTT assay. (E) A flow cytometry assay was conducted to evaluate cell necroptosis induced by $A\beta_{1-42}$ and after treatment with EGb761. (F) The relative expression of the RIP1 protein after treatment with gradient concentrations of EGb761 was determined by Western blotting. *$p < 0.05$, **$p < 0.01$, ***$p < 0.001$ compared to the control group.

Figure 4 Suppression of JNK pathways by EGb761 treatment. (A) The protein levels of JNK/STAT3 signaling pathway proteins were determined by Western blotting. (B) Quantification of (A). *$p < 0.05$, **$p < 0.01$, ***$p < 0.001$ compared to the control group.

Figure 5 Improved cognitive function after EGb761 treatment, as determined by the MWM experiment. (A) The escape latency of the animals on each training session day o across the groups. (B) The average swimming speed of each group. (C) The number of target platform crossings. *$p < 0.05$ compared to the control group.

Figure 6 Rescue of cell death and the suppression of the JNK pathway by EGb761 *in vivo*. (A) IHC was performed in the hippocampal CA1 region of AD rats after EGb761 treatment. (B) The Aβ-stained area was calculated by Image Pro Plus 6.0. (C) Representative Western blotting bands showing the expression of JNK-STAT pathway proteins. (D) Quantification of relative protein expression. *$p < 0.05$, **$p < 0.01$, ***$p < 0.001$ compared to the control group.

Figure 7 A schematic figure illustrates the working model.

Figure S1 (A) Representative bands and quantification of Western blotting showing the expression of protein levels of NCLX, MCUB, MICU1, MICU2, VADC and CV-Sα to investigate effects of EGb761 on mitochondrial calcium efflux. (B) Flow cytometry quantification was performed to determine the cell death (necroptosis and apoptosis) rate after treatment with Cyclosporin A (CsA) or/and EGb761. *$p < 0.05$, **$p < 0.01$ compared to the control group.

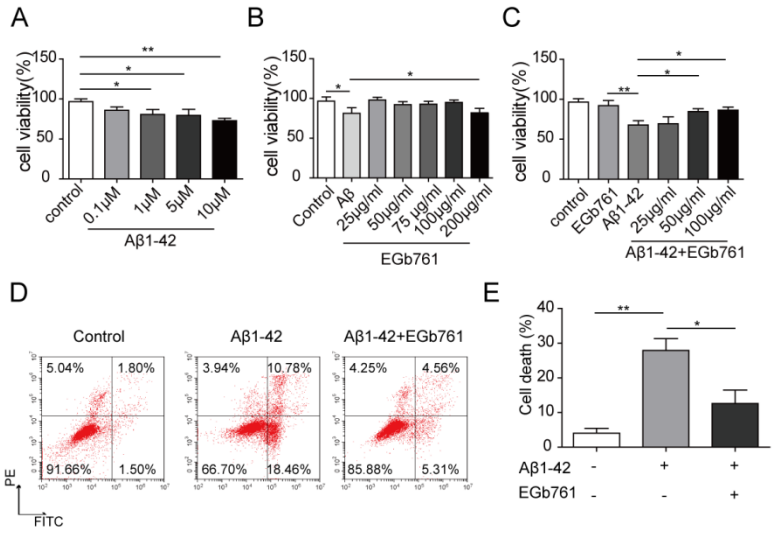

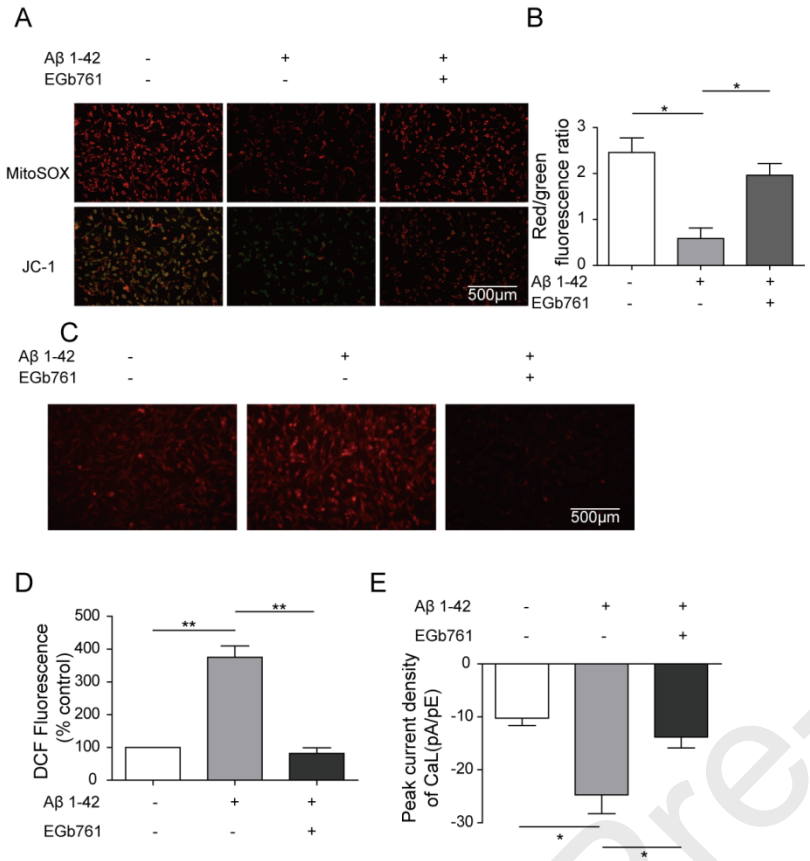

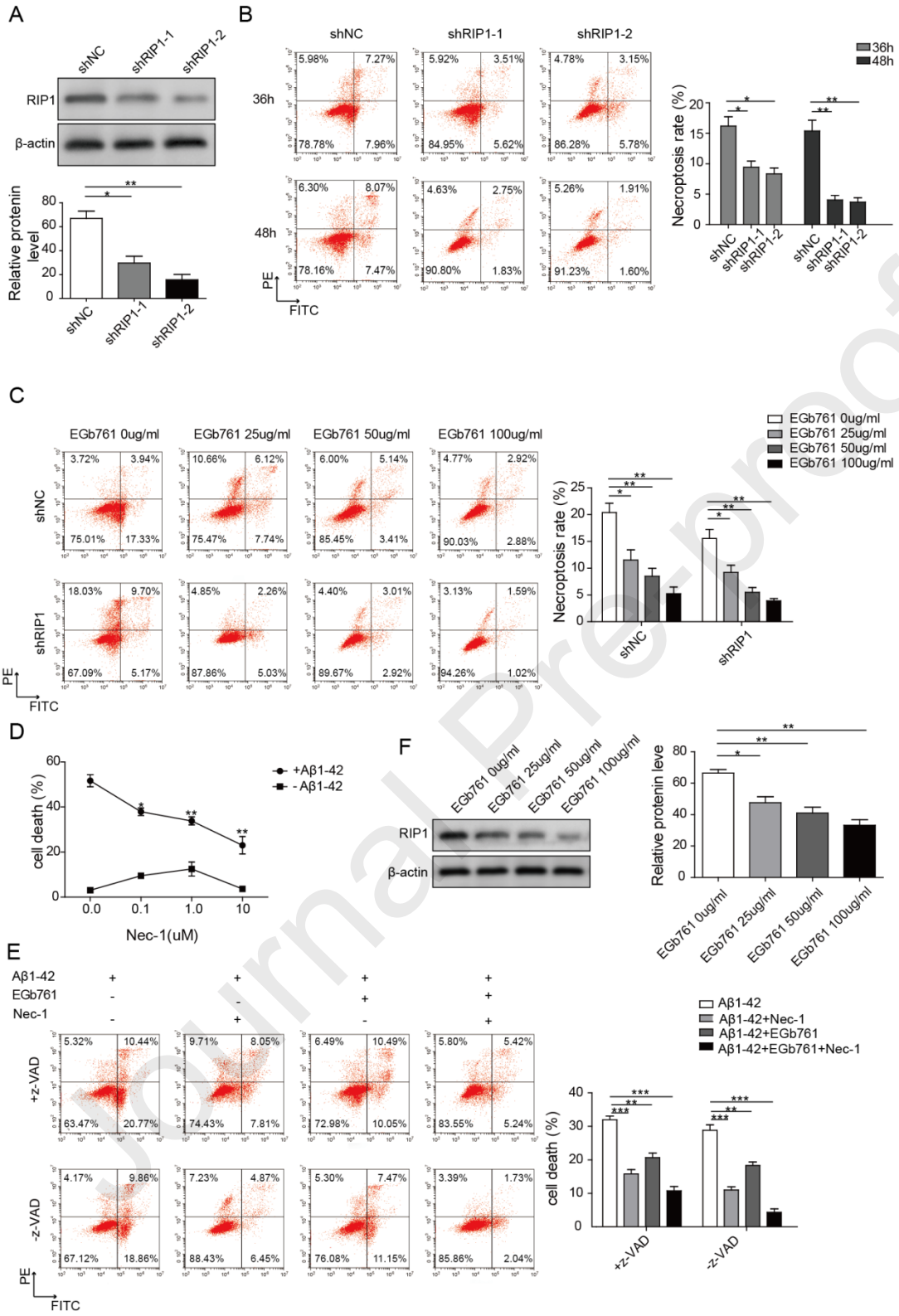

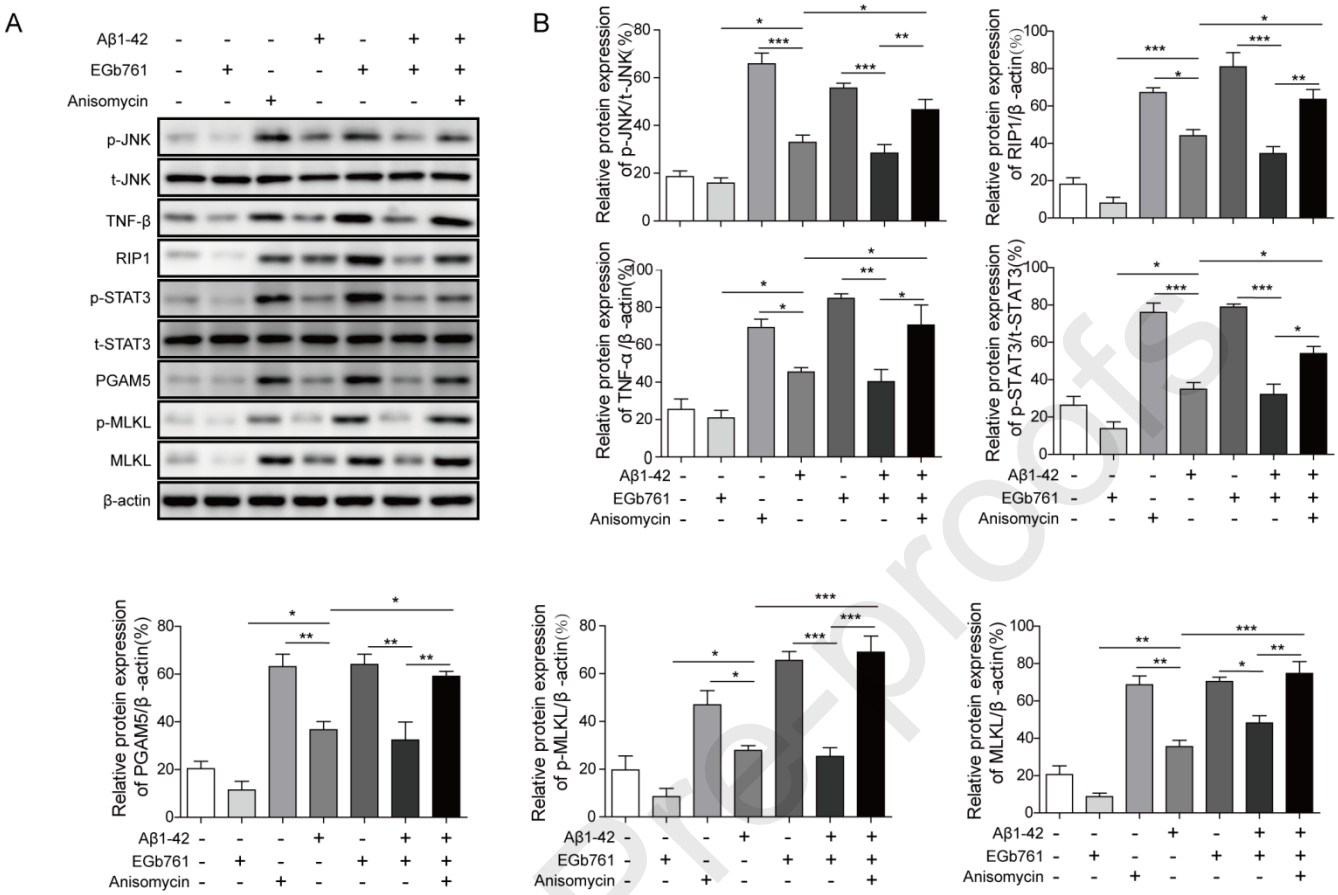

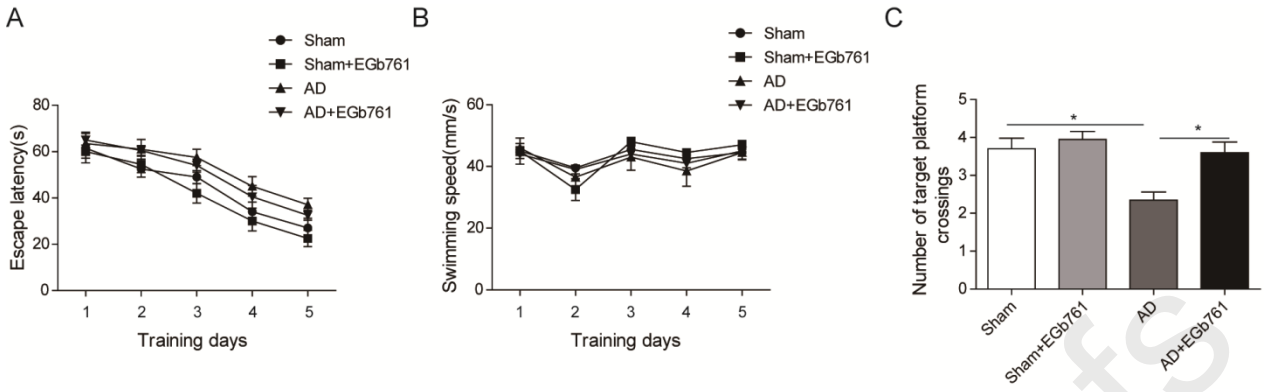

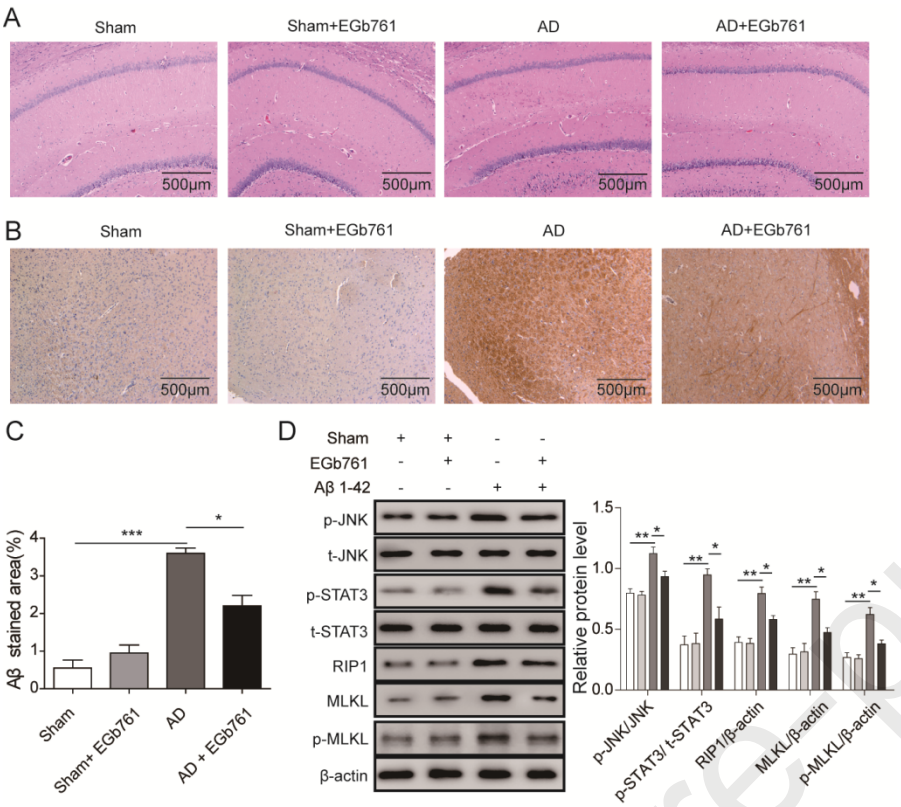

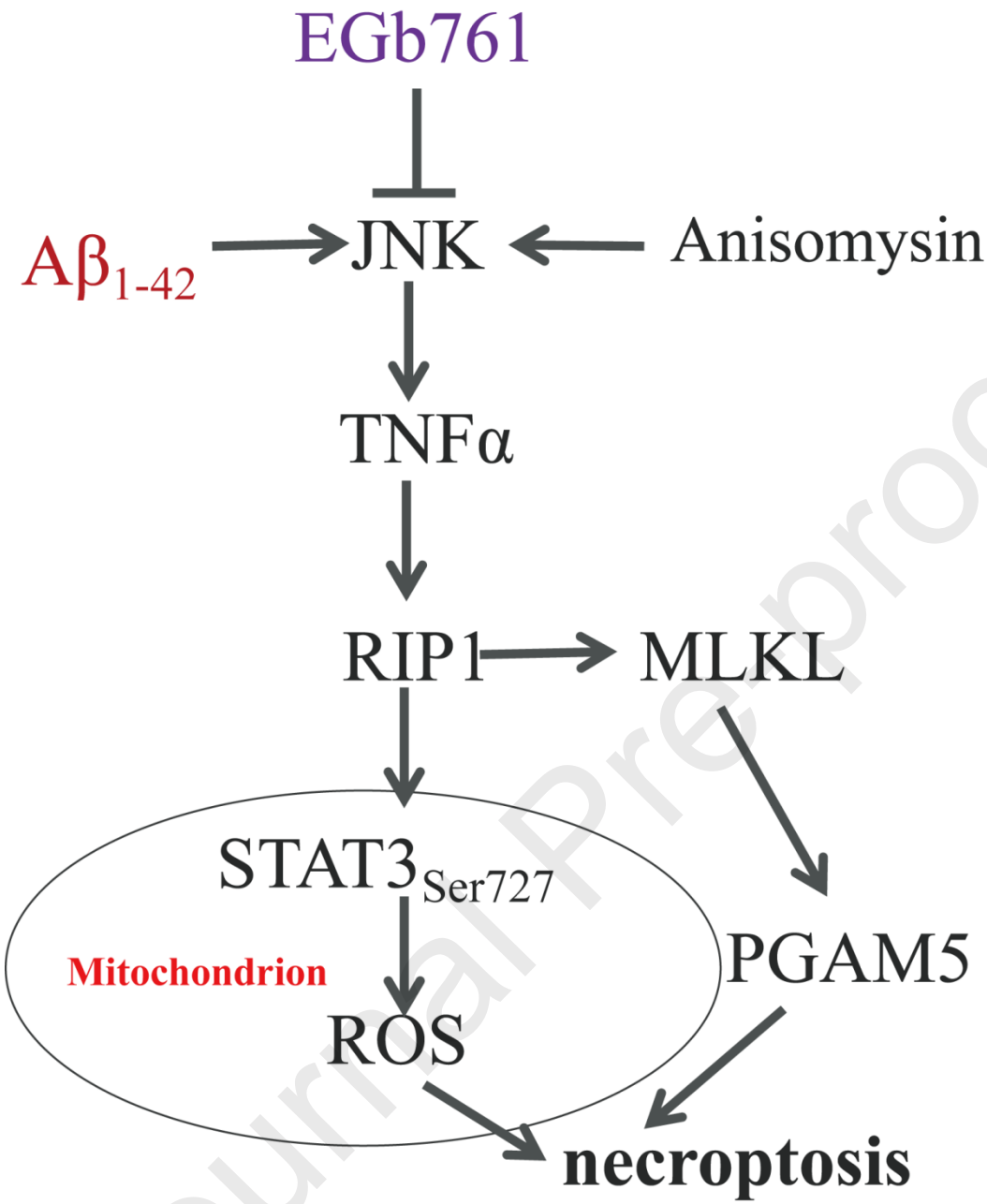

Authors' contributions

ZJC, WPC, GZ and QHL performed experimental studies. ML analysed statistics. JLT designed the study and reviewed the manuscript. XL designed the study, did literature research, prepared, edited and reviewed the manuscript. All authors read and approved the final manuscript.

Highlight

1. Ginkgo extract EGb761 relieves mitochondrial stress of neural cells in AD model.
2. EGb761 intervention rescues spatial memory deficit in AD-model animal.
3. EGb761 rescues cell injury by mediating JNK signal pathway.